Iraqi Journal of Science
ISSN: 0067-2904
GIF: 0.851

# New Pd and Pt Complexes of Guanine –Azo Dye: Structural, Spectroscopic, Dyeing Performance and Antibacterial Activity Studies

**Thanaa J. Al-Hasani*, Zainab S. Almaliky**
Department of Chemistry, College of Science, Baghdad University, Baghdad, Iraq.

**Abstract**

Four new complexes of Pd(II), Pt(II) and Pt(IV) with DMSO solution of the ligand 8-[(4-nitrophenyl)azo]guanine (L) have been synthesized. Reaction of the ligand with Pd(II) at different pH gave two new complexes, at pH=8, a complex of the formula $[Pd(L)_2]Cl_2$.DMSO (1) was formed, while at pH=4.5,the complex$[Pd(L)_3]Cl_2$.DMSO (2) was obtained. Meanwhile, the reaction of the ligand with Pt(II) and Pt(IV) revealed new complexes with the formulas$[Pt(L)_2]Cl_2$.DMSO (3)and $[Pt(L)_3]Cl_4$.DMSO (4) at pH 7.5 and 6 respectively.

All the preparations were performed after fixing the optimum pH and concentration. The effect of time on the stability of these complexes was checked. The stoichiometry of the complexes was determined by the mole ratio and Job methods. The complexes were characterized by micro elemental analysis and molar conductivity together with the magnetic susceptibility measurements. Spectrophotometric measurements, UV-Vis, FT-IR and A.A were also performed. $^1$H NMR spectra for the ligand and $[Pd(L)_3]Cl_2$.DMSO complex were also done. A square planar geometry was suggested for complexes (1) and (3), and octahedral structure for complexes (2) and (4).The Dyeing performance and the antibacterial activities for the ligand and its complexes were also tested.

**Keywords:** Guanine, Azo-dyes, Dyeing performance, Palladium (II), Platinum (II), Platinum (IV), complexes.

# معقدات بلاديوم وبلاتين جديدة لصبغة كوانين– أزو: دراسات تركيبية وطيفية واداء الصبغة والفعالية البايولوجية

**ثناء جعفر الحسني*، زينب صبير المالكي**
قسم الكيمياء، كلية العلوم ، جامعة بغداد ، بغداد ، العراق

**الخلاصة**

حضرت أربعة معقدات جديدة من تفاعل Pd(II) و Pt(II) و Pt(IV) مع الليكاند 8-[(4-nitrophenyl)azo] (L)guanine المذابة في DMSO، لقد اعطى تفاعل Pd(II) مع الليكاند معقدين جديدين في pH مختلف، اذ اعطى عند pH=8 المعقد $[Pd(L)_2]Cl_2$.DMSO(1)، في حين تم الحصول على المعقد $[Pd(L)_3]Cl_2$.DMSO(2) عند pH=4.5. أما تفاعل الليكاند مع Pt(II) و Pt(IV) فقد اعطى معقدين جديدين لهما الصيغتان $[Pt(L)_2]Cl_2$.DMSO (3) و $[Pt(L)_3]Cl_4$.DMSO (4). اجريت جميع التحضيرات بعد تحديد الـ pH الأمثل والتركيز الأمثل. كما تمت دراسة تأثير الزمن على استقرارية المعقدات المحضرة وتم تعيين نسبة الفلز:الليكاند بأستخدام طريقتي جوب والنسبة المولية. لقد شخصت المعقدات بواسطة التحليل الدقيق للعناصر وقياسات التوصيلية الكهربائية والحساسية المغناطيسية. كذلك اجريت القياسات

*Email: thoonjumar@ yahoo.com

الطيفية بأستخدام اطيـــاف اشعة UV–Vis و FT–IR و A.A فضلا عن اجراء تحاليل $^1$H NMR لليكاند ولمعقد $[Pd(L)_3]Cl_2.DMSO$. اقترحت تراكيب المربع المستوي للمعقدين (1) و(3) وتراكيب ثماني السطوح للمعقدين (2) و(4). اختبرت قابلية الليكاند ومعقداته على صباغة الالياف الصوفية والاكريلك ودرست الفعالية البايولوجية لليكاند ولجميع المعقدات.

**Introduction**

Azo compounds are characterized by the presence of azo group (-N=N-), which links two $sp^2$ hybridized carbon atoms . Often , these carbons are part of an extended delocalized electron system involving the aromatic ring , called a chromophore[1-3].They are highly colored that enjoy widespread use as dyes and pigments in a variety of applications that include textile dyeing[4] as well as non-linear and photo electronics[5], especially in optical information storage [6,7]. These compounds are very important molecules and have attracted much attention in both academic and applied research [8,9]. On the other hand, azo compounds are known to be involved in a number of biological reactions, such as inhibition of DNA, RNA and protein synthesis, nitrogen fixation and carcinogenesis [10].They also used as inflammatory, antifungal, and anticancer [11].

Aryl azoimidazole have drawn special attention because of the synthetic simplicity of the system and the biochemical ubiquity of imidazole. The formation of azoimidazole dyes usually involves the reaction between a diazo species with coupling components[12].This class of azo compounds possess active (π-acidic) azo imine, (─N═N─C═N─), function and efficient agents to stabilize low valent metal oxidation states[13]. In addition to their use as analytical reagents[14] and as a staining agents[15], the literature surveys depicts that imidazole derivatives shows various pharmacological activities such as anti viral , anti inflammatory and analgetic , anti depressant , anti fungal and anti – bacterial , anti cancer , anti tubercular and anti leishmanial activity[16].

Guanine is an organic compound belonging to the purine group, a class of compounds consisting of a fused pyrimidine-imidazole ring system, composed of carbon and nitrogen atoms. It is a component of nucleic acids, the cell constituents that store and transmit hereditary traits[17].The first guanine-based difunctional colorimetric receptor 8-[(4-nitrophenyl)azo]guanine (receptor) was designed, synthesized and characterized by IR, UV–Vis,$^1$H NMR and mass spectrometric analysis[18].The receptor was able to recognize Cu(II), Zn(II) and acetate ion through visible color changes in its DMSO and DMSO-$H_2O$ (95:5, v/v) solutions.

The solution of (receptor) underwent visible changes on the respective additions of one equivalent of tetrabutyl ammonium salts of acetate, benzoate and format. Similar additions of M ((II)) as their chloride salts produced a variety of responses.

A series of guanine azo compounds were prepared by Khalaf Y.[19] by coupling of different dizonium salts with guanine. The structures of the prepared compounds were identified by UV-Vis ,IR spectra and elemental analysis.The biological activity of these compouneds were investigated on five genera of pathogenic bacteria: *S.aureus, Str.viridians, Ps.aeruginosa, E.coli and Sh.dysenteria*, using disc diffusion method, showed that these compounds have medium biological effect.

The main target of the present work is to synthesize new complexes of Pd(II), Pt(II) and Pt(IV) with the ligand 8-[(4-nitrophenyl)azo]guanine.The preparation conditions were examined spectroscopically. The complexes were characterized by different physicochemical methods. The dyeing performance of the ligand and its complexes were tested and the antibacterial activities were also studied.

**Experimental**

**Materials:**

All the chemicals used were of analytical reagent grade. They include guanine hydrochloride, p-nitro aniline, potassium tetrachloroplatinat(II), potassium tetrachloropalladate(II) (Fluka). Potassium hexachloroplatinat(IV) (BDH), dimethyl sulphoxide (Biosolve), dimethyl formamide (Merck).

**Physical measurements:**

Elemental analyses and metal contents of the ligand and its complexes were measured using (Euro EA 3000) CHNS analyzer and "GBC 933 $_{Plus}$" Flame Atomic Absorption Spectrophotometer, respectively.IR spectra in the range 4000-200 $cm^{-1}$were recorded on a "Shimadzu F.T.I.R 8400S" Spectrophotometer as CsI discs. The electronic spectra were recorded on "ShimadzuUV-1800" UV-Vis Spectrophotometer.$^1$H NMR spectra were performed by using "Bruker Ultra Shield 300

$MH_Z$"Spectrophotometer. Melting points were measured on "Stuart Melting Point Apparatus". The conductance measurements were carried out using" P.W-9528" Digital Conductometer" HANNA HI 9812 pH/EC/TDS Meter".Magnetic susceptibility was measured at room temperature using "Magnetic Susceptibility Balance Model- M.S.B." Auto Apparatus. The pH of the solution was measured on "JENWAY 3020" pH Meter. The dying performance of the ligand and complexes were tested on "State Company for Woolen Industries in Baghdad using the "Azoic Dyes (the hot dyeing)" method. The antibacterial activity study were done using four types of bacteria, Gram Negative Bacteria , *Escherichia coli*(*E-coli*) , *Proteus mirabillus (pro.)* , and Gram Positive Bacteria, *Staphylococcus aureas* (*Staph*), *Bacillus (Ba.)*. The bacteria were diagnosed and cultured on Eosin Methylene Blue and Moller Hinton Agar medium. The deactivating capacity was tested using the holes method. The holes were saturated with 100µm of $10^{-3}$ M of the given compound and incubated at 37°C for 24 hours.

**Reagents:**

Buffer solutions of acetic acid- ammonium acetate- ammonium hydroxide (0.01M) of pH range (3.5-8.5) were used. The metal ion solutions as ($10^{-2}$-$10^{-4}$) M were prepared by dissolving the appropriate weight of metal salt in the buffer solutions, while the same concentration range of the ligand solutions were also obtained by dissolving the required weight of 8-[(4-nitrophenyl)azo]guanine in DMSO.

**Methods:**

The ligand 8-[(4-nitrophenyl)azo]guanine (L) was prepared following the literature procedure [18] with some modifications. m.p. 270, %yield 73, %Found C 41.297, H 2.892 N 35.112; % calculated C 43.966, H 2.665, N 37.330.

**Synthesis of the Complexes (General method):**

A solution of the appropriate metal salt (0.05mmole) dissolved in the optimum buffer solution (150ml), was added gradually with stirring to a solution of either (1mmole) or (1.5mmole) of the ligand solution in DMSO. The stirring was continued for a period of time. A colored precipitate was obtained. The product was filtered off, washed several times with a 1:1 $H_2O$:EtOH mixture then left to dry. Table-1 describes the data required for the synthesis of the complexes.

**Table 1-** Conditions for the synthesis of azo dye metal complexes

| complex | M:L ratio | gm. of ligand | gm. of metal salt | pH | Stirring time(min.) | ml. DMSO |
|---|---|---|---|---|---|---|
| $[Pd(L)_2]Cl_2$.DMSO | 1:2 | 0.3001 | 0.1632 $K_2PdCl_4$ | 8 | 15 | 150 |
| $[Pd(L)_3]Cl_2$.DMSO | 1:3 | 0.4502 | 0.1632 $K_2PdCl_4$ | 4.5 | 15 | 200 |
| $[Pt(L)_2]Cl_2$.DMSO | 1:2 | 0.3001 | 0.4151 $K_2PtCl_4$ | 7.5 | 60 | 150 |
| $[Pt(L)_3]Cl_4$.DMSO | 1:3 | 0.4502 | 0.2430 $K_2PtCl_6$ | 6 | 60 | 200 |

**Results and Discussion:**

The UV-Vis spectrum of the ligand (L) in DMSO ($10^{-4}$M) within the range 250-1100$cm^{-1}$, displayed mainly two peaks. The first peak appeared at 274nm and was assigned to the moderate energy $\pi\rightarrow\pi^*$ transition of the aromatic rings, while the second broad peak ($\lambda_{max}$) at 498 nm was related to the $\pi\rightarrow\pi^*$ transition of intermolecular charge-transfer taken place through the azo group (-N=N-) [20].

The spectra of an aqueous–DMSO solutions of Pd(II), Pt(II) and Pt(IV) complexes were studied over a wide range of pH and concentrations. A great bathochromic shift (49-59nm) was detected accompanied with color change from red to violet or reddish-violet, which is strongly declaring the interaction of the ligand with the metal ions. Figure -1 shows a comparisons between the UV-Vis spectra of the ligand and of the (Pd(II)-L, Pt(II)-L and Pt(IV)-L) mixed solutions.

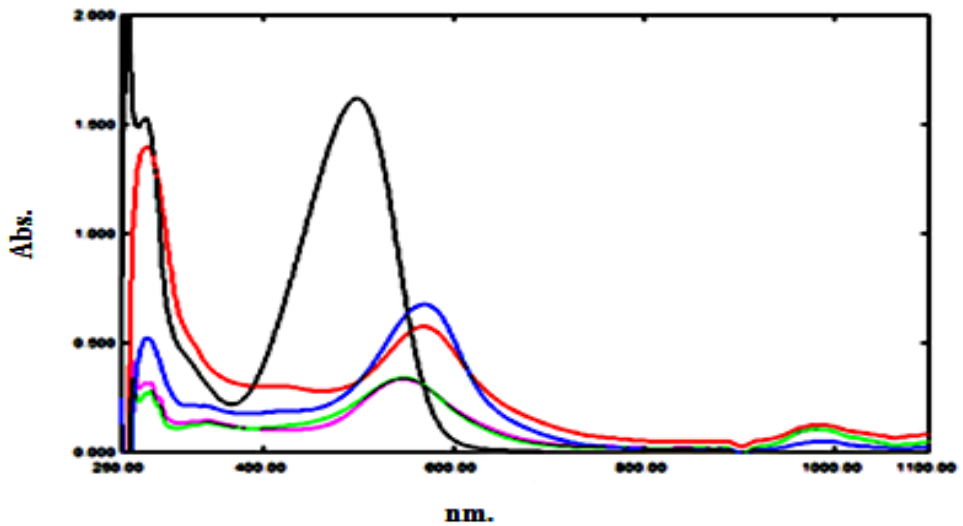


**Figure 1-** The UV-Vis spectra of the mixed solutions of the ligand (L) with: Pd(II) pH 8, Pd(II) pH4.5, Pt(II) pH 7.5 and Pt(IV) pH 6

The UV-Vis spectral study of a wide range of molar concentration ($10^{-2}$-$10^{-4}$) of the metal ion – ligand mixed solutions, revealed that only concentrations of $10^{-4}$ for Pd(II) and Pt(II) and $10^{-3}$M for Pt(IV) solutions obey the Lambert-Beers law. Straight lines with correlation factor, r> 0.920, were obtained when the absorbance was plotted against the molar concentrations($0.25x10^{-4}$-$1.25x10^{-4}$) for Pd(II)and Pt(II) solutions Figure-2,and ($0.25x10^{-3}$-$1.25x10^{-3}$) for Pt(IV) solutions.

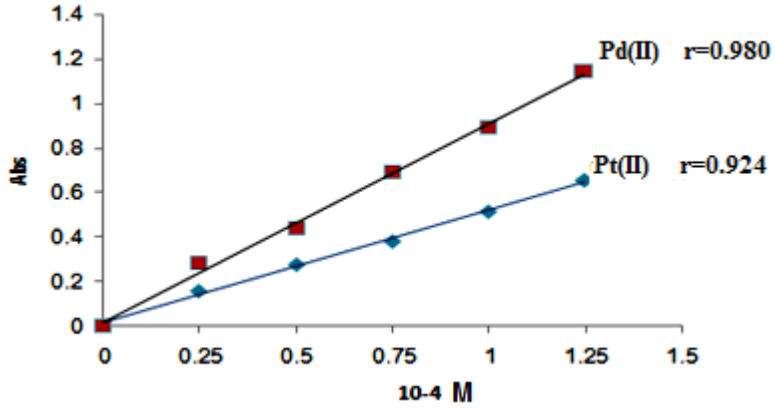


**Figure 2-** Linear relation between molar concentration and absorbance for Pd(II) and Pt(II) complexes

The optimum concentration was chosen for complex solution gave rise to a constant ($\lambda_{max}$) at different pH. The effect of pH was also followed spectroscopically at pH range (3.5-8.5). The absorbance-pH curves for each metal ion at certain $\lambda_{max}$ and concentration are shown in Figure-3.

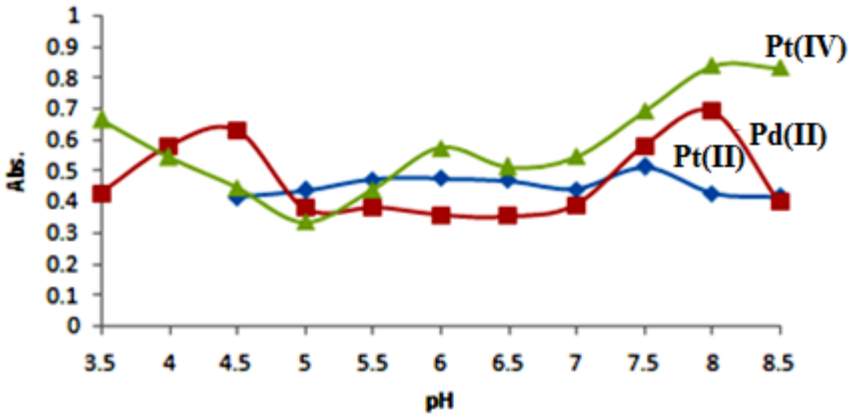


**Figure 3-** Effect of pH on absorbance at $\lambda_{max}$ for Pd(II) ($0.75x10^{-4}$M), Pt(II) ($1x10^{-4}$M) and Pt(IV) ($0.5x10^{-3}$M) -ligand mixed solutions

The Pd(II) curve exhibits two broad plateau represent the presence of two species in solution at pH 4.5 and pH 8. While only one species was recognized in Pt(II) and Pt(IV) solutions at optimum pH 7.5 and 6 respectively. The descending part at the curve may represent the dissociation of the formed complexes. Mole ratio and Job methods [21, 22], were used in order to identify the composition of the complexes formed in solution without isolation. The same results were obtained by the two methods, which suggest a 1:2 M:L ratio for Pd(II) (pH 8) and Pt(II) complexes, and a 1:3 M:L ratio for Pd(II) (pH 4.5) and Pt(IV) complexes. Figures 4 and 5 were selected to represent some of these results.

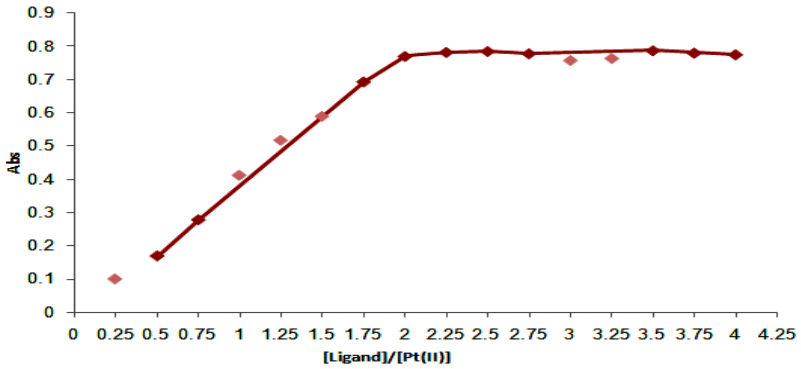


**Figure 4-** Mole ratio plot for Pt(II)-L complex solutions at pH = 7.5 and $\lambda_{max}$ = 565 nm

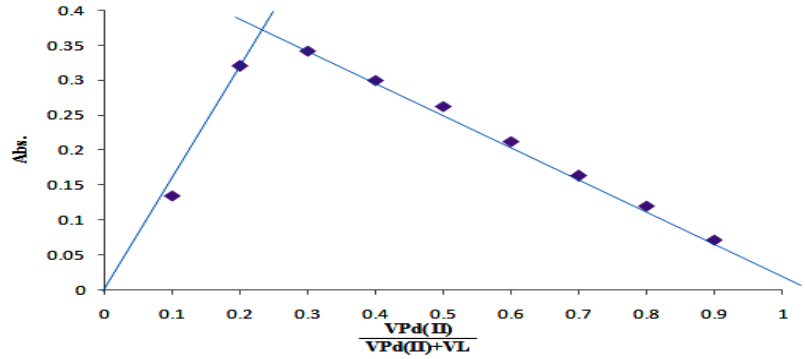


**Figure 5-** Job method of Pd(II)-L complex solutions at pH=4.5 and $\lambda_{max}$ = 547 nm

The effect of time on the development and stability period of the colored complex solutions were also investigated under optimum experimental conditions. The results revealed that the colored complexes started to form after 30-40 min., 10 min., 24 hr. and 9 days for Pd(II) (pH8), Pd(II) (pH4.5), Pt(II) (pH7.5) Figure-6 and Pt(IV) (pH6) Figure-7, complexes respectively.

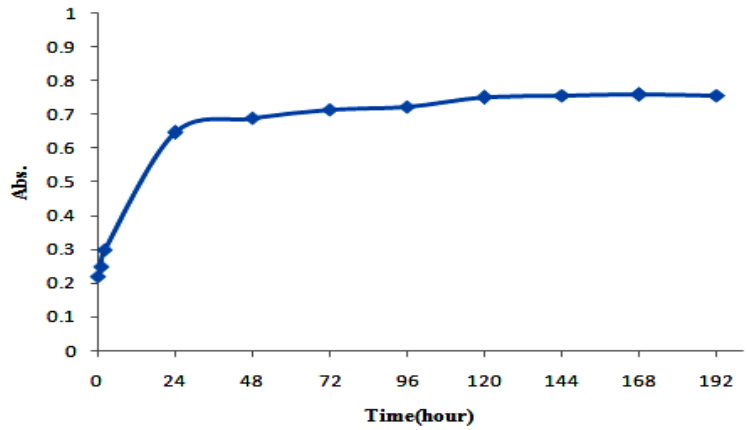


**Figure 6-** Effect of time on stability of Pt(II)-ligand complex solutions at pH = 7.5 and concentration $1x10^{-4}$M

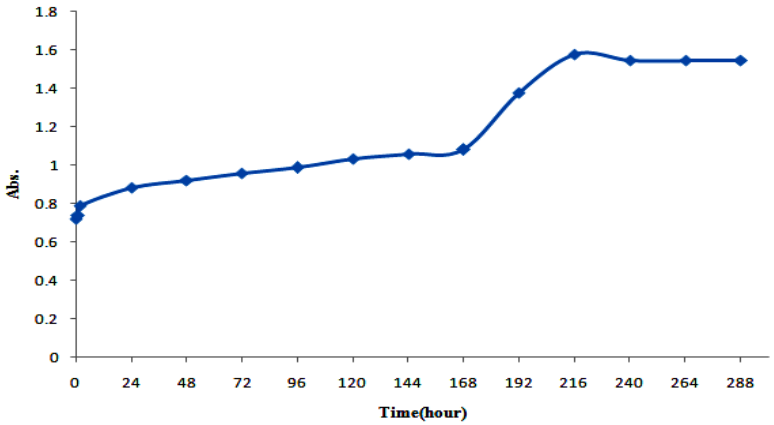


**Figure 7-** Effect of time on stability of Pt(IV)-ligand complex solutions at pH = 6 and concentration $0.5x10^{-3}$ M

The stability constants (K) for Pd(II) and Pt(II) complexes, when the M:L ratio is 1:2, were calculated according to equation (1), while, the stability constants of Pd(II) and Pt(IV) complexes in a 1:3 M:L ratio were calculated according to equation (2)[23].

$$K = \frac{1-\alpha}{4\alpha^3 C^2} \quad \text{..... (1)} \qquad K = \frac{1-\alpha}{9\alpha^4 C^3} \quad \text{..... (2)}$$

$$\alpha = \frac{Am - As}{Am} \quad \text{..... (3)}$$

Where: Am = Absorbance of solution containing excess of ligand, As = Absorbance of solution containing a stoichiometric amount of ligand and metal ion and C= Molar concentration. Table-2 describes the stability constant, optimum molar concentration and time of complex formation.

**Table 2-** Stability constants, optimum molar concentration and time at complex formation

| Complex | Optimum molar conc. | Time of complex formation | As | Am | α | K |
|---|---|---|---|---|---|---|
| $[Pd(L)_2]Cl_2$.DMSO | $0.75x10^{-4}$ | 30-40 min. | 0.400 | 0.682 | 0.413 | $3.738x10^{8}$ * |
| $[Pd(L)_3]Cl_2$.DMSO | $0.75x10^{-4}$ | 10 min. | 0.323 | 0.751 | 0.569 | $1.085x10^{12}$ ** |
| $[Pt(L)_2]Cl_2$.DMSO | $1.00x10^{-4}$ | 1 day | 0.411 | 0.770 | 0.466 | $1.311x10^{8}$ * |
| $[Pt(L)_3]Cl_4$.DMSO | $0.50x10^{-3}$ | 9 days | 0.356 | 1.168 | 0.695 | $1.164x10^{9}$ ** |

*$(L.mol^{-1})^2$, **$(L.mol^{-1})^3$

The solid complexes were prepared by direct reaction of the ligand solution in DMSO with an aqueous solution of the metal ion at optimum pH and certain M:L ratio Table-1. The complexes are quite stable to air. They are insoluble in water and in most organic solvents, but soluble in DMF and DMSO. The molar conductance measurements in DMF ($10^{-3}$ M), revealed that Pd(II) and Pt(II) complexes behave as 1:2 electrolyte while Pt(IV) complex lay in the range 1:4 electrolyte [24]. These results along with the other analytical and spectral data support the molecular formulas of the synthesized complexes $[M(L)_n]Cl_m$.DMSO. When M=Pd(II) (pH 8), Pt(II), n=2, m=2, M=Pd(II) (pH 4.5), n=3, m=2, M=Pt(IV), n=3, m=4. Some physical properties of the synthesized complexes are listed in Table -3.

**Table 3-** Some physical data of the ligand and the new metal complexes

| Compound | Color | M.p. °C | % yield | %Found % (Calculated) | | | | | $\Lambda_m$ ($S.mol^{-1}.cm^2$) |
|---|---|---|---|---|---|---|---|---|---|
| | | | | C | H | N | S | M | DMF |
| $C_{24}H_{22}N_{16}O_7SCl_2Pd$ | Reddish-violet | 330> | 75 | 32.402 (33.653) | 3.182 (2.570) | 25.072 (26.187) | 4.524 (3.739) | 11.55 (12.43) | 155 |
| $C_{35}H_{30}N_{24}O_{10}SCl_2Pd$ | Purple-violet | 310 | 57 | 36.470 (36.333) | 2.843 (2.595) | 29.786 (29.081) | 2.402 (2.768) | 9.031 (9.204) | 170 |
| $C_{24}H_{22}N_{16}O_7SCl_2Pt$ | violet | 278-280 | 74 | 31.965 (30.493) | 2.897 (2.329) | 23.897 (23.728) | 4.837 (3.388) | 20.038 (20.656) | 150 |
| $C_{35}H_{30}N_{24}O_{10}SCl_4Pt$ | Blue-violet | 290-292 | 69 | 31.986 (31.926) | 2.932 (2.804) | 24.859 (25.553) | 2.503 (2.432) | 14.220 (14.829) | 380 |

**$^1$H NMR spectra:**

The $^1$H NMR spectra of the ligand is in a good agreement with that reported by Upadhyay K.K. and co-workers [18]. A comparison between the $^1$H NMR spectra of the ligand Figure-8 and $[Pd(L)_3]Cl_2$.DMSOcomplex, Figure-9 shows that the signal appeared at δ=13.28ppm in the ligand spectrum which assigned to the $–NH_{imidazole}$ proton, was shifted to δ=12.30 ppm in the complex spectra. A singlet signal at δ=11.0ppm in the ligand spectrum belongs to the –NH of pyrimidine proton was splitted toward up field shift δ=10.60 ppm. A third single signal was also observed in the ligand spectrum at δ=7.09 ppm represents the $–NH_2$ group protons. This signal also showed up field splitting δ=6.39 ppm in the complex spectrum. The up field splitting of the proton signals of these groups, Table-4, may reflect the non-involvement of these groups in coordination with the metal ion and in same time supporting the involvement of $N_{pyrim}$ and $N_{azo}$ as a coordination sites.

**Table 4-** Chemical shift (δ, ppm) in $^1$H NMR spectra of the ligand and $[Pd(L)_3]Cl_2$.DMSO complex

| Compound | $-NH_{imidazole}$ | $-NH_{pyrimidine}$ | Ar-H | Ar-H | $-NH_2$ |
|---|---|---|---|---|---|
| L | 13.28 | 11.0 | 8.41 | 8.00 | 7.09 |
| $[Pd(L)_3]Cl_2$.DMSO | 12.30 | 10.60 | 8.41<br>8.29<br>8.24<br>8.19 | 8.03<br>8.02<br>7.72<br>7.60 | 7.09<br>6.39 |

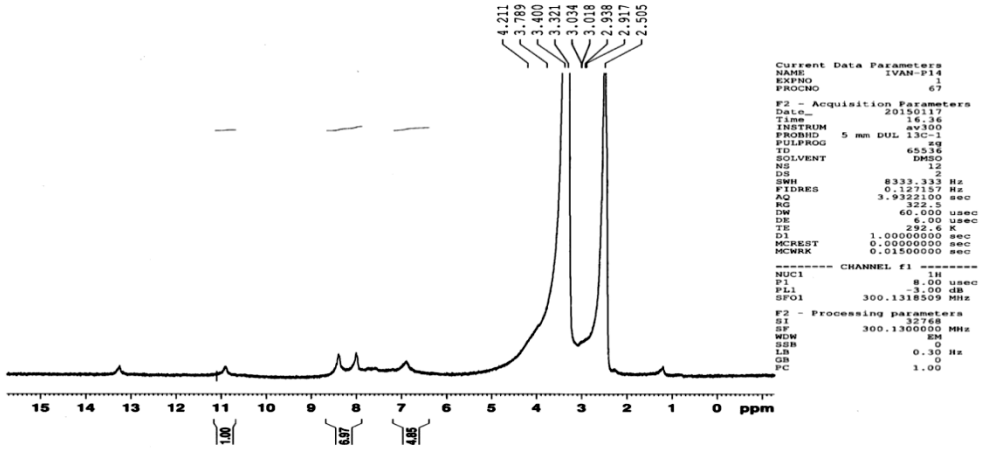


**Figure 8-**$^1$H NMR spectrum of the ligand

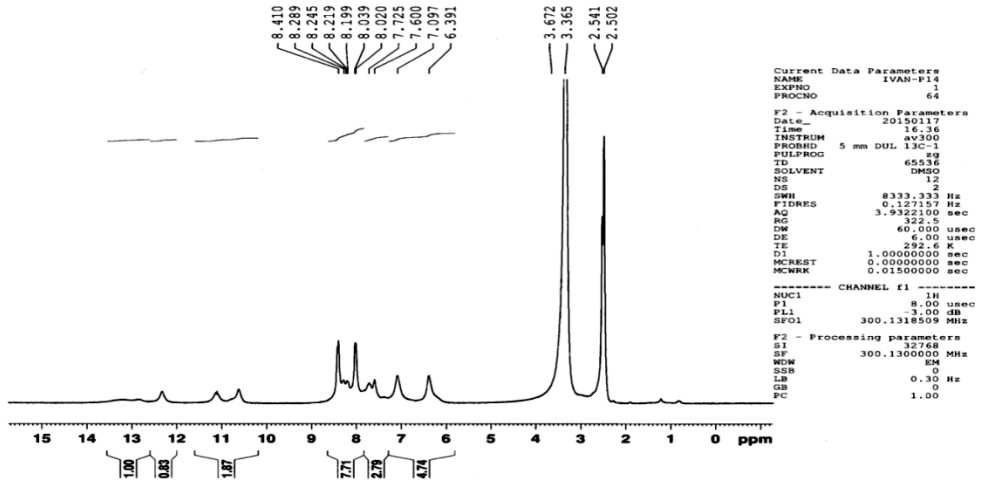


**Figure 9-**$^1$H NMR spectrum of the $[Pd(L)_3]Cl_2$.DMSO complex

**Electronic spectra and Magnetic susceptibility:**

The UV-Vis spectra of the synthesized complexes dissolved in DMSO as $10^{-4}$or $10^{-3}$ M, exhibited strong bathochromic shift of the $\lambda_{max}$ assigned to the $\pi \rightarrow \pi^*$ transition of the ligand.$[Pd(L)_2]Cl_2$.DMSO complex which showed a diamagnetic property. This will suggest a low-spin square planar geometry

for this complex. One weak peak was observed in the electronic spectrum of this complex at 915nm (10900 $cm^{-1}$) which may belongs to the $^1A_1g \rightarrow {}^1B_1g$ transition [25]. The spectrum of $[Pt(L)_2]Cl_2$.DMSO complex (Figure10) which also gave low $\mu_{eff}$ value, showed two weak peaks at 993 nm (10070 $cm^{-1}$) and 917 nm (100905 $cm^{-1}$), may be due to $^1A_1g \rightarrow {}^1A_2g$ and $^1A_1g \rightarrow {}^1B_1g$ transitions respectively. These transitions are responsible for the square planar geometry. The low $\mu_{eff}$ value may also confirm this configuration. In the meanwhile, $[Pd(L)_3]Cl_2$.DMSO complex exhibited three d-d transitions in the electronic spectrum. The three peaks were observed at 993 nm (10070 $cm^{-1}$), 917 nm (10905 $cm^{-1}$)and 881 nm (11350 $cm^{-1}$), Figure-11.The first and second peaks, may belong to the transition $^3A_2g_{(F)} \rightarrow {}^3T_2g_{(F)}$ $\nu_1$. The splitting of this peak may be pointed out for the presence of some Z-out distortion among the Z-axis perpendicular on the square planar base of the octahedral. The third peak may be assigned to the $^3A_2g_{(F)} \rightarrow {}^3T_1g_{(F)}$ $\nu_2$ transition, while the transition $^3A_2g_{(F)} \rightarrow {}^3T_2g_{(p)}$ $\nu_3$ which usually appears in the range (29455-2515 $cm^{-1}$) may be obscured by the ligand peak. The $\mu_{eff}$ value for this complex (2.605 B.M.) Table-5, is approaching the value of octahedral six-coordinate high-spin geometry[24]. The d-d transitions expected for $d^6$ Pt(IV) octahedral complexes in the visible region are, $^1A_1g \rightarrow {}^1T_1g$, $^1A_1g \rightarrow {}^1T_2g$ and the forbidden transition $^1A_1g \rightarrow {}^3T_1g$[26]. In the present work, two peaks were observed in the $[Pt(L)_3]Cl_4$.DMSO spectrum at 887 nm (1127 $cm^{-1}$) and at 982 nm (10183 $cm^{-1}$) which were assigned to the transitions $^1A_1g \rightarrow {}^1T_1g$ and the spin-forbidden transition $^1A_1g \rightarrow {}^3T_1g$ respectively. The other expected transition $^1A_1g \rightarrow {}^1T_2g$ was not observed because of the interfering with the strong ligand peak at 571 nm (17513 $cm^{-1}$).

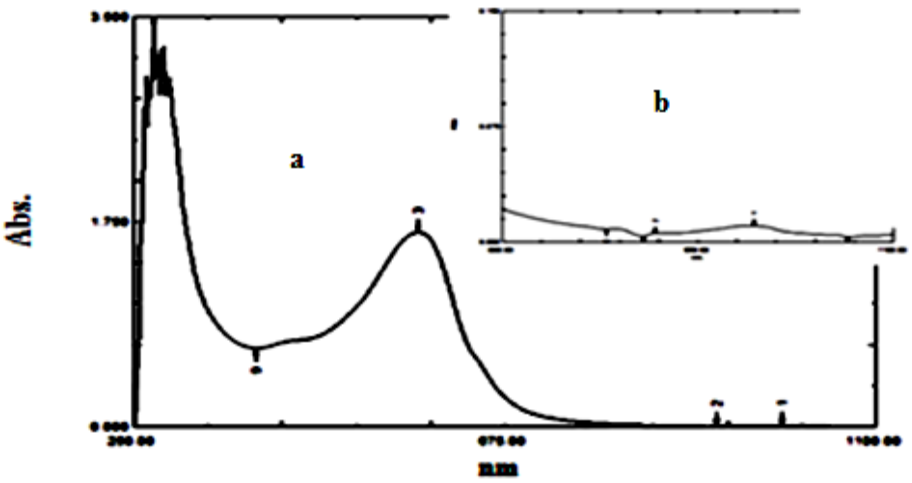


**Figure 10**- UV-Vis spectra of $[Pt(L)_2]Cl_2$.DMSO a- at $10^{-4}$M b- d-d transitions at $10^{-4}$

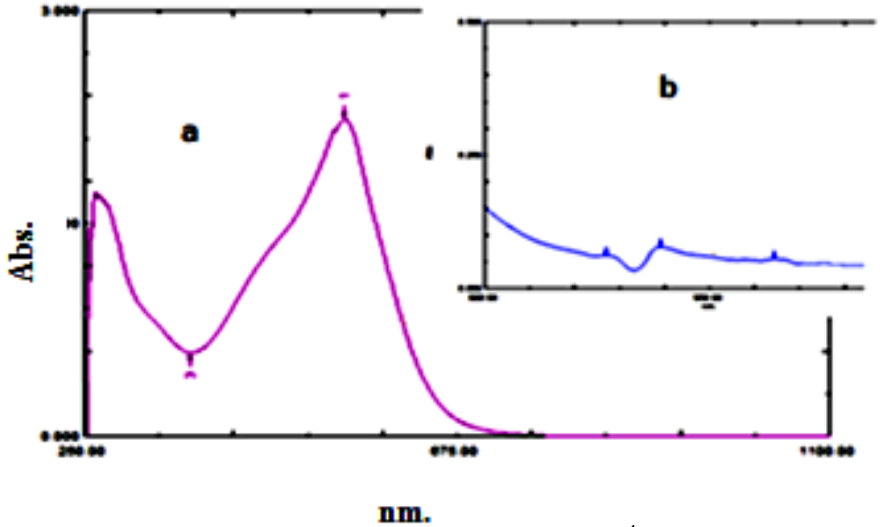


**Figure 11**- UV-Vis spectra of $[Pd(L)_3]Cl_2$.DMSO at a- $10^{-4}$M, b- d-d transition at $10^{-3}$M

**Table 5-** Wave length, magnetic susceptibility and molar extinction coefficient (ε) for DMSO solution of metal complexes

| Compounds | Molar Conc. | λnm | Wave Number $cm^{-1}$ | $\varepsilon_o x10^4$ $L.mol^{-1}$ $cm^{-1}$ | Assignment | $\mu_{eff}$ |
|---|---|---|---|---|---|---|
| 8-[(4-nitrophenyl) - azo]guanine | $1x10^{-4}$ | 498<br>274 | 20080<br>36496 | 1.619<br>1.528 | $\pi\rightarrow\pi^*$ Int. cha. trans.<br>$\pi\rightarrow\pi^*$ tran. arom. ring | zero |
| $[Pd(L)_2]Cl_2.DMSO$ | $1x10^{-3}$<br>$1x10^{-4}$ | 915<br>557<br>228 | 10928<br>17953<br>43859 | 0.005<br>1.581<br>2.445 | $^1A_1g\rightarrow{}^1B_1g$<br>$\pi\rightarrow\pi^*$ Int. cha. trans.<br>$\pi\rightarrow\pi^*$ tran. arom. ring | zero |
| $[Pd(L)_3]Cl_2.DMSO$ | $1x10^{-3}$<br><br><br>$1x10^{-4}$ | 993<br>917<br>881<br>547<br>230 | 10070<br>10905<br>11350<br>18281<br>43478 | 0.005<br>0.007<br>0.006<br>2.234<br>2.006 | $^3A_2g_{(F)}\rightarrow{}^3T_2g_{(F)}$<br>$^3A_2g_{(F)}\rightarrow{}^3T_1g_{(F)}$<br>$^3A_2g_{(F)}\rightarrow{}^3T_2g_{(F)}$<br>$\pi\rightarrow\pi^*$Int.-cha.-trans.<br>$\pi\rightarrow\pi^*$tran. arom. ring | 2.605 |
| $[Pt(L)_2]Cl_2.DMSO$ | $1x10^{-4}$ | 993<br>917<br>566<br>272<br>235 | 10070<br>10905<br>17667<br>36764<br>42553 | 0.011<br>0.006<br>1.658<br>3.416<br>1.633 | $^1A_1g\rightarrow{}^1A_2g$<br>$^1A_1g\rightarrow{}^1B_1g$<br>$\pi\rightarrow\pi^*$Int.-cha.-trans.<br>$\pi\rightarrow\pi^*$ tran. arom. Ring<br>$\pi\rightarrow\pi^*$tran. arom. ring | zero |
| $[Pt(L)_3]Cl_4.DMSO$ | $1x10^{-4}$ | 982<br>887<br>571<br>276<br>228 | 10183<br>11273<br>17513<br>36231<br>43859 | 0.088<br>0.042<br>1.058<br>1.864<br>1.280 | $^1A_1g\rightarrow{}^3T_1g$<br>$^1A_1g\rightarrow{}^1T_1g$<br>$\pi\rightarrow\pi^*$Int. cha. trans.<br>$\pi\rightarrow\pi^*$ tran. arom. ring<br>$\pi\rightarrow\pi^*$ tran. arom. ring | zero |

**FT-IR Spectra and mode of bonding:**

The FT-IR spectra of the synthesized complexes in CsI were compared with that of the prepared ligand. The spectra of the complexes showed the absorption bands characteristic of the ligand with some differences ascribed to the formation of respective ion associated. The most characteristic infrared spectral bands of the free ligand and its complexes are listed in Table-6.

The most significant informations on the geometry of these complexes comes from the analysis of the imidazole, the azo bridge and the $-NH_2$ absorption regions. The ligand showed a triplet band at 3392, 3336 and 3303 $cm^{-1}$, assigned to the ν(N-H) for $NH_2$ group[27]. This band remained unaltered in the complexes spectra, indicating no coordination through the nitrogen of the $NH_2$ group. The little change in position of these triplets, sometimes, is presumably due to the increasing or decreasing of their-sharpness. This can be confirmed by the presence of the unchangeable strong-sharp δ (NH) band at 1585 $cm^{-1}$[28]. A doublet band at 3130 and 3118 $cm^{-1}$ in the ligand spectrum corresponding to the ν (N-H) of the secondary amines[29],again the change in positions, sometimes, may be due to the broadening of the bands. The band at 1697 $cm^{-1}$in the ligand spectrum which refers to the ν(C=O) [30], did not show any change in position or intensity in the complexes spectra, which supports the non – coordination of this group with the metal ion. The ν(N=N) was observed in the ligand spectrum as a strong band at 1423 $cm^{-1}$.This band represents a characteristic feature of the azo compounds [31]. The intensity of this band was diminished in the complexes spectra while a new band appeared at lower frequency, ~1392 $cm^{-1}$. No change in the $\nu(C-N)_{NH}$ of the imidazole ring at 1334$cm^{-1}$ was detected in the complexes spectra, while a remarkable change was observed for the medium doublet shoulder ν(C=N) at 1660 and 1637 $cm^{-1}$. This may be a good indication for the participation of nitrogen atom of the (C=N) group of imidazole but not the nitrogen of the (N−H) group [32].A number of new bands not presented in the free ligand spectrum were observed in the range 450-200 $cm^{-1}$. The presence of the $\nu(M-N)_{azo}$, and $\nu(M-N)_{Imid.}$[33] support our results about the coordination sites of the ligand with metal ions. Figures-12 and 13 show the FT-IR spectra of the ligand and $[Pd(L)_3]Cl_2$.DMSO complex respectively.

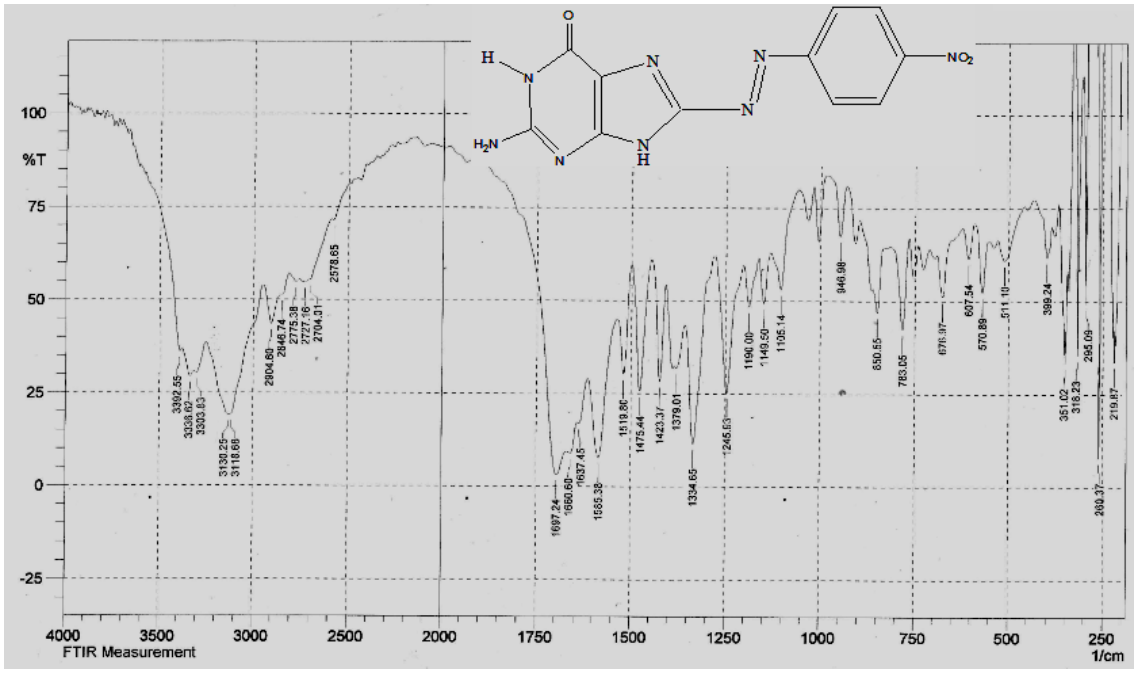


**Figure 12-** FTIR spectrum of azo ligand (L)

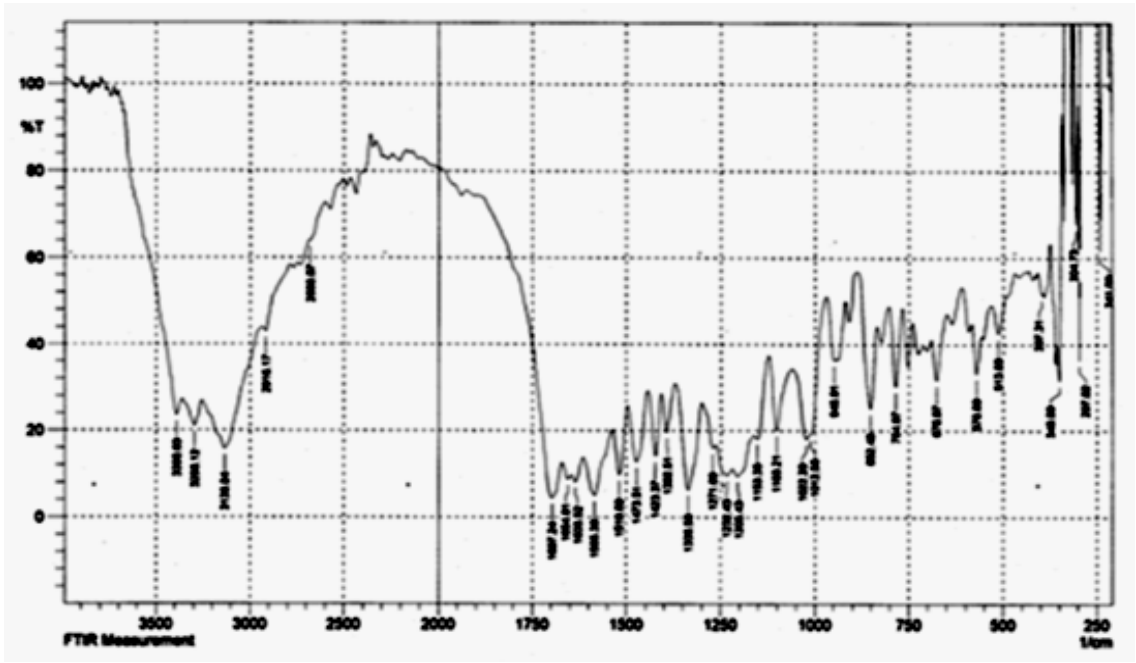


**Figure 13-** FTIR spectrum of $[Pd(L)_3]Cl_2$.DMSO complex.

**Table 6-** Selected FT-IR spectral bands ($cm^{-1}$) of ligand and its metal complexes

| Compound | ν (N–H)$_{NH2}$ | ν (N–H)$_{NH}$ | ν (C=N) | δ(N–H)$_{NH}$ | ν (N=N) | ν (N=N)+ δ(C–N=N–C) | M–N$_{oxo}$ | M–N$_{im}$ | Other bands ν ($NO_2$) | DMSO ν(S=O)[34] |
|---|---|---|---|---|---|---|---|---|---|---|
| L | 3392<br>3336<br>3303 } s.trip. | 3130 } v.s.<br>3118 } d. | 1660 } m.d<br>1637 } sh. | 1585 s. | 1423 s. | 1190<br>1149<br>1105 } m.tri. | ---- | ---- | 850 s. | ----<br>---- |
| $[Pd(L)_2]Cl_2$. DMSO | 3332<br>3313 | 3211 } br.<br>3114 } m. | 1635 s. | 1589 s. | 1427 v.w. | 1101 s. | 374 w. | 275 m. | 854 s. | ----<br>1026 m. |
| $[Pd(L)_3]Cl_2$. DMSO | 3390 s.sharp.<br>3296 | 3138 s. | 1654 } s.d<br>1635 } | 1585 s. | 1423 m.<br>1392 m. | 1103 s. | 349 m. | 304 m. | 852 s. | ----<br>1022 } v. s.d.<br>1012 } |
| $[Pt(L)_2]Cl_2$. DMSO | 3375<br>3330<br>3305 } str.trip | 3167 } s.br<br>3141 } d. | 1633 s. | 1587 s. | 1425 m.<br>1392 w. | 1101 m. | 437 w. | 300 m. | 854 s. | ----<br>1022v. s. |
| $[Pt(L)_3]Cl_4$. DMSO | 3394<br>3332<br>3305 } str.trip. | 3132 s. | 1654 } s.d.<br>1637 } | 1585 s. | 1425m.<br>1392 m. | 1151 } w.d.<br>1110 } | 441 w. | 297 m. | 856 s. | 1944 v.w.<br>1060 } v.s.d.<br>1029 } |

s.= strong, m.=medium, w=weak, d.= doublet, trip.=triplet , sh.=shoulder , br.=broad

On the basis of the analytical and spectroscopic data obtained, the following chemical structures Figure-14 may be proposed for the synthesized complexes.

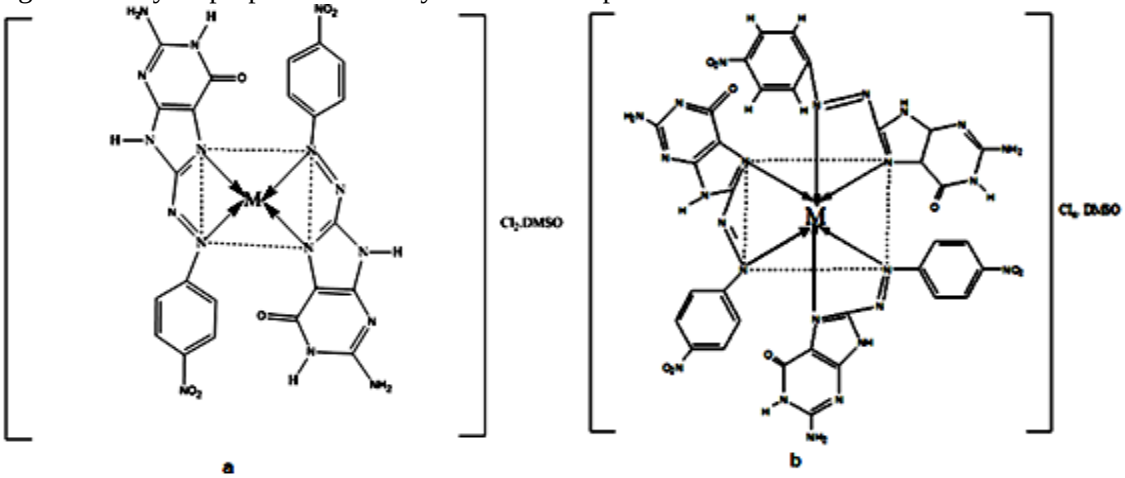


**Figure 14-** The suggested structures of a- $Pd(L)_2]Cl_2$.DMSO and $[Pt(L)_2]Cl_2$.DMSO, b- $Pd(L)_3]Cl_2$.DMSO and $[Pt(L)_3]Cl_4$.DMSO

## Dyeing properties

The dyeing performance of the ligand and its complexes were applied on wool and acrylic fabric. These dyes provided colors in the range of orange, red, light-violet, blue-violet and grey Figure-15 with good brightness and depth on the fabric.

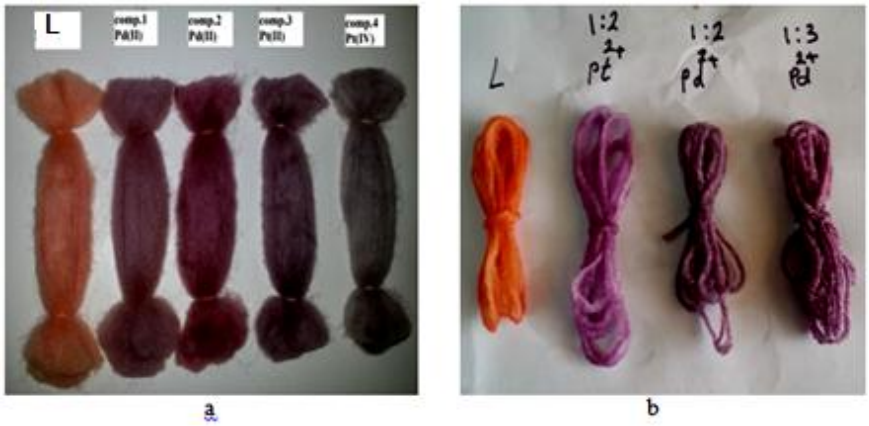


**Figure 15-** Dyeing of a- 100% wool and b- 100% acrylic by the ligand and its complexes

## Antibacterial activity

The antibacterial activity for the ligand and the synthesized complexes were studied against four selected types of bacteria. DMSO was used as a solvent and as a control Metronidazole was used as a standard material. The zone of inhibition of bacterial growth around the disc for one of the $^{-}$G and $^{+}$G specimen of bacteria are presented in Figure 16 and the data are listed in Table-7. In general, the data revealed that the complexes showed a relatively strong deactivating capacity against the $^{+}$G *Staphylococcus aureus* and $^{-}$G *Proteus mirabillus* specimen. Different deactivating capacity was recorded for $^{+}$G *Bacillus* and $^{-}$G *Escherichia coli* specimen of bacteria. However, introduction of metal in complexes increase the deactivating capacity of the ligand. Finally, the ligand and the complexes showed stronger deactivating capacity in comparison with the Metronidazole standard.

**Table 7-** Diameters (cm) of deactivation of bacteria of the ligand and its complexes

| No. | Compound | G+(Staph.) | G+(Ba.) | G-(E-coli) | G-(Pro.) |
|---|---|---|---|---|---|
| 1 | $[Pd(L)_3]Cl_2$.DMSO | 1.9 | 1.2 | 2.3 | 2.9 |
| 2 | $[Pd(L)_2]Cl_2$.DMSO | 1.3 | 1.0 | 2.0 | 2.6 |
| 3 | $[Pt(L)_3]Cl_4$.DMSO | 1.4 | 1.5 | 1.2 | 2.0 |
| 4 | $[Pt(L)_2]Cl_2$.DMSO | 1.5 | 1.2 | 1.7 | 1.7 |
| 5 | Ligand | 1.2 | 1.3 | 1.3 | 1.3 |
| 6 | Metronidazole | 0.7 | 3.5 | 0.8 | 0.8 |

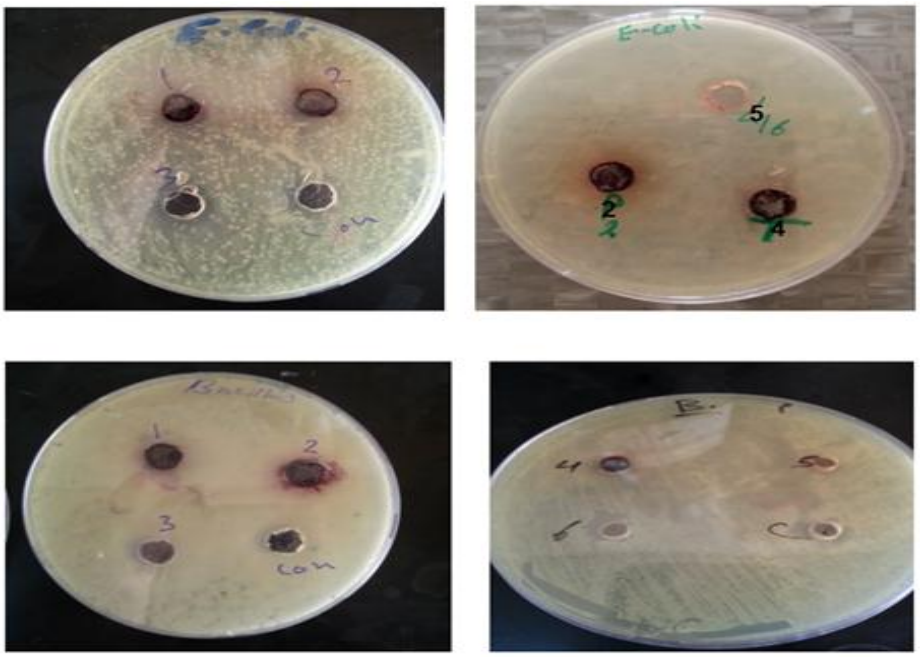

**Figure 16**-Antibacterial activity of ligand and its complexes against($G^-$) bacteria(*E.coli*) and ($G^+$) bacteria *Ba.* 1-$[Pd(L)_3]Cl_2$.DMSO, 2-$[Pd(L)_2]Cl_2$.DMSO, 3-$[Pt(L)_3]Cl_4$.DMSO, 4-$[Pt(L)_2]Cl_2$.DMSO, 5-ligand. 6-Metronidazole, C-DMSO (control).

## Conclusions

We have shown in this work that the ligand 8-[(4-nitrophenyl)azo]guanine was acted as a neutral bidentate chelating ligand. The ligand is coordinated with Pd and Pt ions through the azo nitrogen and the imidazole ring nitrogen. Two complexes of Pd(II) ion were obtained at different pH media, while, one complex with Pt(II) and Pt(IV) was obtained. Fine shiny colors were observed by testing the dyeing performance of the ligand and complexes on wool and acrylic. The in-vitro antibacterial study for the ligand and its complexes showed a strong deactivating capacity against certain bacteria specimen.

## References


1. Blumel, S., Knackmuss, H. and Stolz, A.**2002**. Molecular cloning and characterization of the Gene coding for the aerobic azoreductase from xenophilusazovorans. *App. Env. Micr.*, 68(8), pp: 3948-3958.
2. Mohammed, I. A. and Mustapha, A. **2010**.Synthesis of new azo compounds based on N-(4-Hydroxypheneyl) maleimide and N-(4-Methylpheneyl) maleimide. *Molecules*, 15, pp: 7498-7508
3. Zarei, A., Hajipour, A. R., Khazdooz, L., MirjaliliB. F. and Chermahini, A. N. **2009**.Rapid and efficient diazotization and diazo coupling reaction on silica sulfuric acid under solvent-free conditions. *Dyes and Pigments*, 81(3),pp: 240-244.
4. Koh, J. and Greaves, A. J. **2001**.Synthesis and application of an alkali-clearable azo disperse dye containing a flurosulfonyl group and analysis of its alkali-hydrolysis kinetics. *Dyes and Pigments*, 50(2), pp: 117–126.
5. Abdallah, S.M. **2012**.Metal complexes of azo compounds derived from 4-acetamidophenol and substituted aniline. *Arabian Journal of Chemistry.* 5,pp: 251–256
6. Li, X., Wu, Y., Gu, D. and Gan, F.**2009**.Optical characterization and blue-ray recording properties of metal(II) azobarbituric acid complex films. *Mat. Sci, Eng. B.*, 158(3), pp: 53–57.
7. Sabi, Y., Tamada, S., Iwamura, Oyamada, T., Bruder, M., F., Oser, R., Berneth, H. and Hassenruck, K. **2003**.Development of organic recording media for blue high numerical aperture optical disc system. *J. Appl. Phys*. 42, pp: 1056–1058.
8. Li, X., Wu, Y., Gu, D. and Gan, F. **2010**.Spectral, thermal and optical properties of metal(II)–azo complexes for optical recording media. *Dyes and Pigments*, 86(2),pp: 182–189.
9. Nishihara, H. **2004**.Multi-mode molecular switching properties and functions of azo-conjugated metal complexes. *Bull. Chem. Soc. Jpn*., 77, pp: 407–428.

**10.** Badea, M., Olar, R., Cristurean, E., Marinescu, D., Emandi, A., Budrugeac, P., Segal, E. **2000**.Thermal stability study of some azo-derivatives and their complexes, Part 2. New azo-derivative pigments and their Cu(II) complexes. *J. Therm. Anal. Calor*, 77(3),pp: 815–824.

**11.** Yildiz, E. and Boztpe, H. **2002**.Synthesis of novel acidic mono azo dyes and investigation of use in the textile industry. *Turk. J. Chem.*, 26, pp: 897-903.

**12.** Mamdouh, S.M., Swasan, S.H., Alaa E. A., Nessma, M. N. **2012**.Synthesis and spectroscopic characterization of gallic acid and some of its azo complexes. *J. Mol. Struct*, 1014,pp: 17-25.

**13.** Hemang, M., Yogesh, K.S. and Ashish R. S. **2013**. Azo group containing bis ligand and its coordination polymers. *Res. J. Chem. Sci*., 3(1), pp: 48-56.

**14.** Nushiravan, K. and Gulu. G. **2014**. Determination of Manganese with 2,2-dipyridyle and 2,4-dinitrobenzolazosalicylic acid in standard sample of the alloy "BANRO A185", *J. Chem. Eng. Chem. Res*., 1(2),pp:110-113.

**15.** El-Sonbati, A., Diab, M., Belal, A. and Morgan, Sh. **2012**. Supramolecular structure, mixed ligand and substituents effect on the spectral studies of oxovanadium (IV) complexes of bioinorganic and medicinal relevance. *Spectrochim. Acta*. , 95, pp: 627–636.

**16.** El-Sonbati, A., Diab, M., Belal, A. and Morgan, Sh. **2013**.Coordination chemistry of supra molecular Rhodanineazo-dye sulphadrugs, *Review. Inorg. Chim.*, 404, pp: 175–187.

**17.** Betitana, V. **1983**. *The Chemistry and Biology of Antibiotic*. Second Edition. Elsevier Scientific Publishing Comp. Amsterdam.

**18.** Upadhyay, K., Kumar, A., Zhao J. and Mishra, R. K. **2010**. Naked-eye recognition of Cu(II),Zn(II) and acetate ion by the first guanine-based difunctional chromoinophore. *Talanta*, 8, pp: 714–721.

**19.** Khalaf, Y. **2008**. Synthesis a number of azo compounds derived from guanine and studying their biological activity on pathogenic bacteria. *J. of Al-Anbar University for Pure Science*, 2(3), pp: 150-157.

**20.** Saha, S., Majumdar, T. and Mahapatra, A. **2006**. Kinetic and mechanistic studies of the interaction of 2-mercapto pyridine with dichloro [1-alkyl-2-(arylazo) imidazole] palladium(II) complexes.*Transition Met. Chem*., 31,pp: 1017-1023.

**21.** Abas, A. **2007**. Synthesis and spectroscopic study of Ni(II) , Pd(II) , Pt(II) and Pt(IV) Complexes with New Thiazolylazo Ligands. Ph.D. *Thesis*, Department of Chemistry, College of Science, University of Baghdad. Iraq, Baghdad.

**22.** Kumar, B., Kanchi, S., Bisetty, K. and Jyothi, N. V. **2014**. Analytical and biological evaluation of two Schiff's bases: spectrophotometeric analysis of copper (II) in water and soil samples. *J. Environ. Anal. Chem.*, 1, pp:1-7

**23.** Hussan, A.**2009**. New study of the extracting of liquid-liquid for Iron (II) and (III) using the extractor of N-acetyl DL-Tryptophan. *Journal of Kerbala University*, 7(3), pp: 72-82.

**24.** Jambi1, S. and Kandil, S. **2012**. Synthesis and characterization of Ni(II), Pd(II), Pt(II) complexes of N-allyl-N'-(4-methylthiazol-2-yl)thiourea. *J. Mater. Environ. Sci.* 3 (3), pp: 591-604.

**25.** Paola, D., Luca, P, Davide, E, Laura, M. and Angela, S. 2010. Square-planar $d^8$ metal mixed-ligand dithiolene complexes as second order nonlinear optical chromophores: Structure/property relationship. *Coordination Chemistry Reviews*, 254, pp: 1434-1447.

**26.** Greenwood, N. and Earnshaw, A. **1998**. *Chemistry of Elements*. 2nd .Ed. Pergamon Press In.

**27.** Nag, J., Pal, S. and Sinha C. **2005**. Synthesis and characterization of palladium(II) and silver(I) complexes of antipyrine-azo-imidazole. *Trans. Met. Chem.*30, pp: 523-533.

**28.** Byabartta, P., Jasimuddin, S. and Sinha, C. **2004**. Synthesis, spectral characterization and redox properties of heterolepticruthenium (II)–ptolylazoimidazole–pyridine complexes. *Indian J. Chem*., 43A, pp: 737-747.

**29.** Ranjan, S. and Dikeshit, S. **2000**. Synthesis and reactivity in inorganic and metal-organic chemistry. *Inorg.Met. Org. Chem*., 30, pp: 1039-1049.

**30.** Sarker, K., Halder, S., Banerjee, D., and Mondal, K. **2010**. Copper-thioarylazoimidazole complexes: structures, photochromism and redox interconversion between Cu(II),Cu(I) and correlation with DFT calculation. *Inorganica Chimica Acta*., 363, pp: 2955-2964.

**31.** Nag, J. K., MisraT. K. and Sinha, C. **1997**. Synthesis, characterization and electrochemical studies of dioxouranium(VI) complexes of dioxolenes with pyridine bases. *Indian J. Chem.*, 36, pp: 951-961.

**32.** Banerjee, D., Ray U., Chantrapromma, S., Fun, H., Lin, J., Lun, T. and Sinha C. **2005**. Cobalt(II)-azoimidazole complexes : Structures of $[Co(MeaaiMe)_4](ClO_4)_2.H_2O$ and $[Co(HaaiMe)_2(NCS)_2]$ (MeaaiMe = 1-methyl-2-(p-tolylazo)imidazole; HaaiMe= 1-methyl-2-(phenylazo)imidazole). *Polyhedron*, 24(9), pp: 1071-1078.

**33.** Dinda, J., Jasimuddin, S., Mostafa, G. Hung, C. and Sinha C. **2004**. Silver(I) complexes of the naphthyl-azoimine function: single crystal X-ray structure of bis-[1-ethyl-2-(naphthyl-α-azo)imidazole]silver(I) perchlorate. *Polyhedron*, 23(5), pp: 793-800.

**34.** Shundalau, M., Chybirai, P. and Komyak, A. **2012**.Structure and vibrational IR spectra of a $UCl_4 \cdot 2DMSO$ complex. *Journal of Applied Spectroscopy*, 79(2), pp:165-172